Available online at www.sciencedirect.com
SCIENCE DIRECT®
Physics Letters B 615 (2005) 167–174
PHYSICS LETTERS B
www.elsevier.com/locate/physletb

^{16}O Coulomb dissociation: towards a new means to determine the $^{12}C + \alpha$ fusion rate in stars

F. Fleurot [a,1], A.M. van den Berg [a], B. Davids [a,2], M.N. Harakeh [a], V.L. Kravchuk [a,3], H.W. Wilschut [a], J. Guillot [b], H. Laurent [b], A. Willis [b], M. Assunção [c,4], J. Kiener [c], A. Lefebvre [c], N. de Séréville [c,5], V. Tatischeff [c]

[a] *Kernfysisch Versneller Instituut, Zernikelaan 25, 9747 AA Groningen, The Netherlands*
[b] *IPN, 15 rue Georges Clemenceau, 91406 Orsay cedex, France*
[c] *CSNSM, bat. 104-108, 91405 Orsay Campus, France*

Received 21 April 2004; received in revised form 8 March 2005; accepted 13 April 2005

Available online 25 April 2005

Editor: V. Metag

Abstract

A feasibility study was made of an important aspect of the Coulomb-dissociation method, which has been proposed for the determination of the rate of the astrophysically important $^{12}C(\alpha,\gamma)^{16}O$ reaction. A crucial aspect is the disentanglement of nuclear and Coulomb interactions on one hand and the separation of dipole and quadrupole contributions on the other. As a first step the resonant breakup via two well-known 2^+ states of ^{16}O was measured. The differential cross section of $^{208}Pb(^{16}O, ^{16}O^*)^{208}Pb$ and the angular correlations of the fragments ^{12}C and α in the center of mass were measured and compared to theoretical predictions calculated in DWBA and the coupled-channel method. The best agreement was found for the state at 11.52 MeV associated to a one-step excitation from the ground state, while the 9.84 MeV requires coupling to the first-excited 2^+ state and is not well described.

PACS: 97.10.Cv; 26.20.+f; 24.10.Eq; 27.20.+n; 25.70.De; 25.60.Gc

Keywords: Stellar structure, interiors, evolution, nucleosynthesis, ages; Hydrostatic stellar nucleosynthesis; Coupled-channel and distorted-wave models; Nuclei with $6 < A < 19$; Coulomb excitation; Breakup and momentum distributions

E-mail addresses: fleurot@snolab.ca (F. Fleurot), wilschut@kvi.nl (H.W. Wilschut).

[1] Present address: Department of Physics, Laurentian University, Sudbury, ON, P3E 2C6, Canada.

[2] Present address: TRIUMF, 4004 Wesbrook Mall, Vancouver, BC, V6T 2A3, Canada.

[3] Present address: INFN, Laboratori Nazionali di Legnaro, Viale dell'Universita 2, 35020 Legnaro (PD), Italy.

[4] With financial support from CNPq, Brazilian Government Agency; present address: Departamento de Fisica Nuclear, Institute de Fisica da Universidade de São Paulo, São Paulo, Brazil.

[5] Present address: Centre de Recherche du Cyclotron, UCL, 2, B-1348 Louvain-la-Neuve, Belgium.

0370-2693
doi:10.1016/j.physletb.2005.04.035

The $^{12}C(\alpha,\gamma)^{16}O$ reaction is known as one of the most important nuclear reactions in astrophysics, and remains one of the most challenging to study. Despite many experimental efforts to measure direct radiative capture (see in particular [1–7]), our knowledge of its cross section is still unsatisfactory. Measurements have been carried out down to a center-of-mass energy of $\epsilon = 1$ MeV with relatively low statistics, requiring uncertain extrapolation of the fusion excitation function down to $\epsilon = 300$ keV, i.e., the astrophysically relevant region. The uncertainty is due to the many different mechanisms that contribute.

A promising alternative to direct measurements is the Coulomb-dissociation method (see in particular [8–12] and [13] for a complete review). This method highly favors the E2 component and appears to be complementary to the ^{16}N β-delayed α-decay technique that allowed the estimation of the E1 contribution [14,15].

A complicating aspect is the uncertainty in the nuclear interaction amplitude interfering with the Coulomb part of the interaction. Moreover, one must disentangle the dipole and quadrupole contributions. Measuring Coulomb breakup at $\epsilon \approx 300$ keV all complications occur simultaneously. Therefore, as an intermediate step we have studied the dissociation via two well-known 2^+ states in ^{16}O. This restricts the problem to the nuclear-Coulomb interference. However, such measurements at larger center-of-mass energies $\epsilon \sim 4$ MeV require a spectrograph with large angular opening and momentum bite, as we will discuss below. The Big Bite Spectrometer (BBS) at KVI fulfills this requirement. Our result clearly indicates the crucial role of the nuclear part of the interaction and the additional steps required for a reliable measurement in the astrophysically relevant energy region.

The Coulomb-dissociation experiment was carried out on the well-known 2^+ states at 9.84 MeV (2_2^+; $\epsilon = 2.68$ MeV) and 11.52 MeV (2_3^+; $\epsilon = 4.36$ MeV) in ^{16}O. The aim was twofold: first, to test the possibility to fit the angular distributions with distorted-wave Born approximation (DWBA) or coupled-channel (CC) calculations that include the nuclear and Coulomb interactions and the interferences between their contributions; second, to measure the angular correlations of the fragments in the breakup center of mass. It has been shown [8,10,11] that the angular correlation of the fragments is very sensitive to the interference between the contributions of the various multipolarities involved in the excitation process. Therefore, a measurement of the angular correlation of the fragments is an important requirement to separate the E1 and E2 contributions in the ^{16}O continuum.

Two experiments were carried out. For the first experiment, the superconducting cyclotron AGOR at KVI provided a 60 MeV/u ^{16}O beam to bombard a 7.8 mg/cm^2 ^{208}Pb target. The final experiment used an 80 MeV/u ^{16}O beam, and a 4 mg/cm^2 ^{208}Pb target to reduce straggling effects. At these energies there is a sufficiently high yield of virtual photons for a high excitation cross section. The experimental detection technique exploits the fact that the relative energy of the α and ^{12}C particles in the moving $^{16}O^*$ frame is small. In the laboratory frame their velocities are approximately equal to the beam velocity. The magnetic rigidities of the particles are also close because of the same mass-to-charge ratio $A/q = 2$ for both α and ^{12}C (see Fig. 1). Both particles could then be detected in the spectrometer where their relative momentum could be measured. In nearly all cases of elastic breakups (without target excitation), the magnetic rigidity of one fragment is slightly above the magnetic rigidity of elastically scattered ^{16}O particles, while the other is slightly below. When the nominal rigidity of the spectrometer is set to the rigidity of elastically scattered ^{16}O particles, the fragments can simultaneously be detected in the scintillator paddles on the left and right sides of the nominal rigidity, respectively.

As shown in Fig. 1, a high beam velocity reduces the angular opening between the fragments in the laboratory frame, as well as the momentum bite, and increases the chance to detect both fragments simultaneously. Moreover, an important aspect of the experiment is the measurement of the fragment angular correlations in the center-of-mass frame. A large acceptance, therefore, allows the measurement of the correlations following the breakup via the 2^+ states located at relatively high excitation energy. The B-mode of the BBS has large acceptances in both angular opening (10 msr) and momentum bite (19%) and is therefore well suited for this type of measurement [16].

The BBS ion-detection system [17] consisted of two cathode-strip chambers (CSC's) for position and angle measurements. These were placed in a vacuum

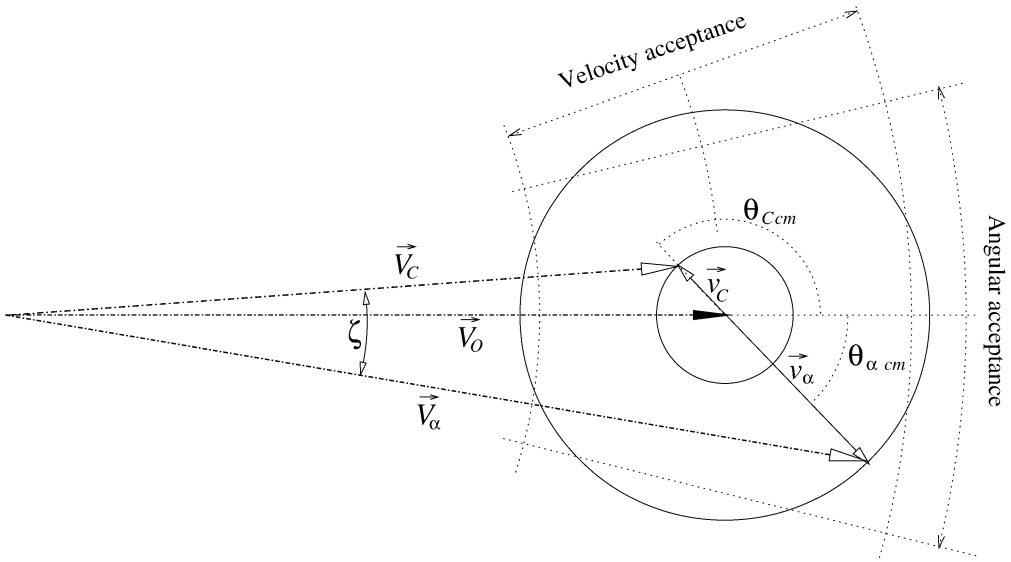

Fig. 1. For a given oxygen scattering angle, the limiting factors are the spectrometer angular and momentum (or equivalently velocity) acceptances, $\vec{v}_{\mathrm{C}}$ and $\vec{v}_\alpha$ are the velocities in the breakup center of mass of ^{12}C and α, $\vec{V}_{\mathrm{C}}$ and $\vec{V}_\alpha$ are their velocities in the laboratory frame, ζ is the angle between $\vec{V}_{\mathrm{C}}$ and $\vec{V}_\alpha$, $\vec{V}_{\mathrm{O}}$ is the velocity of ^{16}O in the laboratory, i.e., the velocity of the center of mass and $\theta_{\mathrm{C\,cm}}$ and $\theta_{\alpha\mathrm{cm}}$ are the breakup polar angles of the fragments in the $^{16}\mathrm{O}^*$ center of mass. ($\phi_{\mathrm{C\,cm}}$ and $\phi_{\alpha\mathrm{cm}}$, not shown for clarity, are the out of plane angles.)

chamber, with the first one positioned at the BBS focal plane and the second 30 cm further downstream. Outside the vacuum chamber, scintillator paddles placed downstream measured the time of flight and energy loss of the light ions. A coincidence between the scintillator paddles was used as the trigger condition for the experiment. In this configuration, the elastically scattered ^{16}O particles arrived near the center of the focal plane, where they were stopped with a narrow brass finger to avoid high count rates and random coincidences.

The time of flight through the BBS and the energy loss of each fragment in the scintillator paddles provided full particle identification. In this way ^{12}C–α coincidences were distinguished from other coincident fragmentation products. The measurement of the positions and angles of the fragments in the spectrometer focal plane by the CSC's allowed the calculation of their trajectories through the spectrometer. The reconstruction of the angular correlations of the fragments in the breakup center of mass and of the angular distribution of the $^{16}\mathrm{O}^*$ particles before breakup in the laboratory was carried out via a ray-tracing matrix containing the empirical ion-optical parameters of the BBS.

For natural parity states, the excited ^{16}O nucleus decays into α and ^{12}C in their 0^+ ground states. However, two 2^- states in ^{16}O, lying at 12.53 MeV and 12.97 MeV, can only decay to the first-excited state of ^{12}C (2^+, 4.44 MeV), because a transition to the ground state is parity-forbidden. In this case, these events appear in the region of interest of the relative-energy spectrum. However, we could remove these events because the sum of the kinetic energies of the fragments plus the Q-value of the reaction is nearly equal to the beam energy for decays to ground states, while this is 4.44 MeV lower for decays to the first-excited state of ^{12}C. The ^{208}Pb recoil energy is about 200 keV. The sum-energy spectrum also allowed the discrimination of mutual-excitation events, i.e., when the target is also excited. Thus to measure breakup at relative high energies is not as demanding as for the astrophysically relevant small energies. In the BBS configuration, the optimal resolution in ϵ is determined by the angular resolution in the opening angle ζ. An average resolution of 5 mrad can be achieved; at $\epsilon = 400$ keV this means a resolution of 40 keV. However, at these small energies other issues such as track separation become increasingly important, and were not part of the present study.

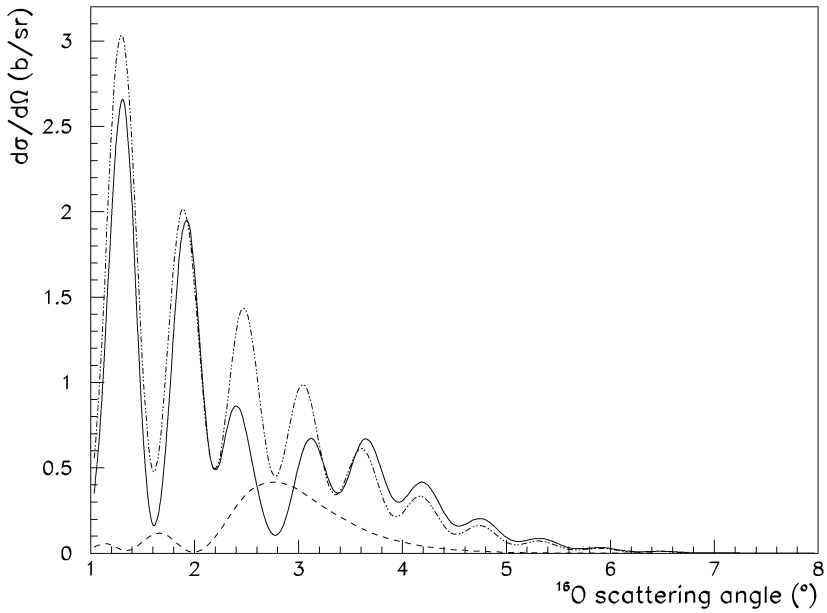

Fig. 2. The calculated angular differential cross section of ^{16}O excited to the 2^+ resonance at 11.52 MeV for a beam energy of 80 MeV/nucleon. The dotted line is a pure nuclear calculation, the dashed line is pure Coulomb, and the solid line includes both interfering interactions.

To elucidate the role of the nuclear and Coulomb processes and their interference, separate calculations for either contribution were made, the details will be discussed later. The result is shown in Fig. 2. The maximum Coulomb contribution occurs near the ^{16}O scattering angle of 3°, where a strong interference occurs with the nuclear contribution that dominates elsewhere. The BBS was set at an angle of 3°.

To make comparisons between the experimental data and calculations, three different projections were made in view of the limited statistics. These are the angular distribution of the reconstructed $^{16}O^*$ and the correlations in the scattering plane $W_{\theta_{\mathrm{C\,cm}}}$ (to be referred to as W_θ) and out of the scattering plane $W_{\phi_{\mathrm{C\,cm}}}$ (to be referred to as W_ϕ). Here $\theta = 0$ corresponds to the direction of the $^{16}O^*$ particle and $\phi = 0$ to its reaction plane (left side). In particular the strongly varying acceptance for the reconstructed $^{16}O^*$, further complicated by some poorly functioning sections of the focal plane detectors, did not allow to construct an acceptance and efficiency corrected $^{16}O^*$ angular distribution. Instead the following strategy was adopted: the results of DWBA and CC calculations performed with the code ECIS [18] were sampled in a Monte Carlo event simulation that takes into account the specific efficiency and acceptance of the setup (details are in Ref. [19]). The 2^+ state at 9.84 MeV is known to be populated via a coupling with the 2^+ state at 6.92 MeV [20]. Therefore, coupled-channel calculations were necessary to calculate the differential cross section for the state at 9.84 MeV. The DWBA and CC calculations were carried out with the optical-model potential parameters determined in Ref. [21] from elastic scattering of 94 MeV/u ^{16}O on ^{208}Pb. We made the usual assumption of equal deformation lengths for each potential. The sampling took into account the angular correlations of the fragments calculated from the m-substate population with the S-matrix elements computed by ECIS. The obtained differential distributions of ^{208}Pb(^{16}O, $^{16}O^*$)^{208}Pb for both 2^+ resonances are shown in Fig. 3. The simulations also provide predictions for the angular correlations of the fragments in the center of mass. The results are plotted for both states in Figs. 4 and 5, respectively.

In the following we discuss the comparison between data and calculations. First we note the impact of the nuclear contribution in the calculated angular distributions. The CC and DWBA calculations predict different interference patterns, indicating the importance of a correct description. The overall agreement is

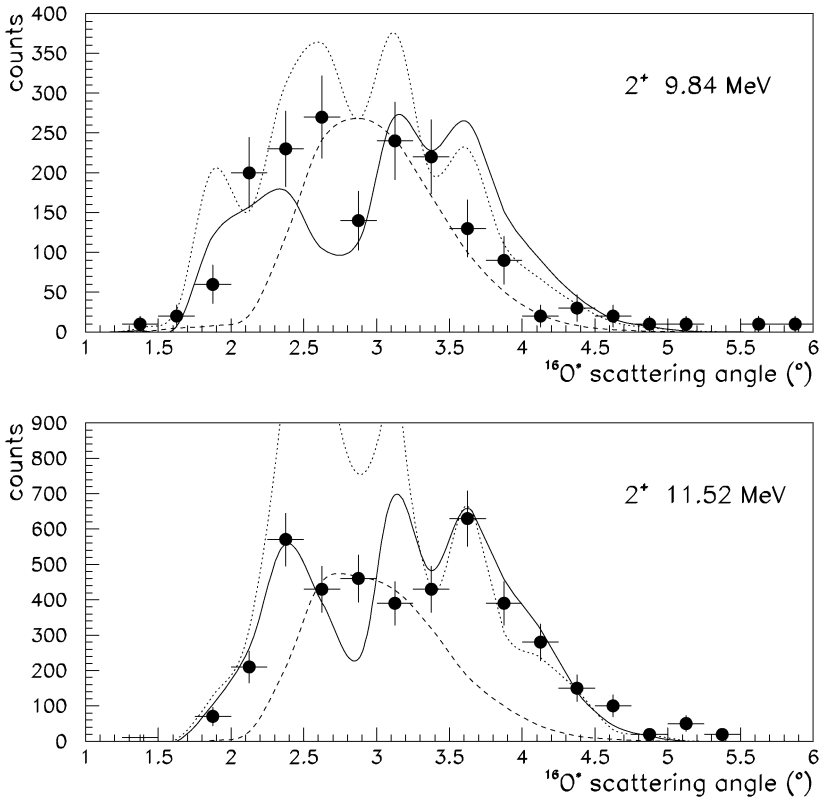

Fig. 3. Angular distributions of $^{16}O^{*}$ for both 2^{+} states. The data points are from the final experiment, the lines are from the Monte Carlo sampling of the ECIS calculations described in the text. The lines are marked the same way as in Fig. 2. The differential cross sections for the states at 9.84 MeV and 11.52 MeV were calculated with CC and DWBA, respectively. The average angular resolution is about 0.3°.

best for the state at 11.52 MeV (bottom Figs. 3 and 5). The minimum χ^2 in fitting the angular distribution gave a deformation length of $\delta = 0.083 \pm 0.003$ fm, only about 5% lower than the value extracted from literature [22]. This would correspond to a 10% error in the reduced transition probability and thus in the cross section. This is actually comparable to the systematic error in the normalization of the data, which was estimated to be 7%. Therefore, the integrated cross section over the investigated region is well measured. It also supports strongly that the DWBA calculations describe the excitation process including both Coulomb and nuclear interactions and their interferences. Therefore, this implies that the method can be used to measure the deformation parameters and to deduce the reduced electromagnetic transition probabilities $B(\mathrm{E}L)$.

Figs. 4 and 5 show that the angular correlations W_θ are reproduced if not very accurately for the points at 55° and 65° in both cases. Both angular correlations W_ϕ display the typical quadrupole distribution pattern. The state at 11.52 MeV is nearly perfectly reproduced. The state at 9.84 MeV shows a yield twice too strong for three points around 180°, while it is relatively good at other angles. The fact that populating this state requires a complex excitation process might be the reason why this is not perfectly reproduced by the calculations. However, the low-energy continuum of ^{16}O is excited directly from the ground state with little contributions from any coupled channels [20], therefore this should not be an issue for future experiments aiming to measure at excitation energies of relevance for stellar burning.

As a further check calculations for both states were carried out using the folded-potential model. In this model a collective $L = 2$ transition density of the

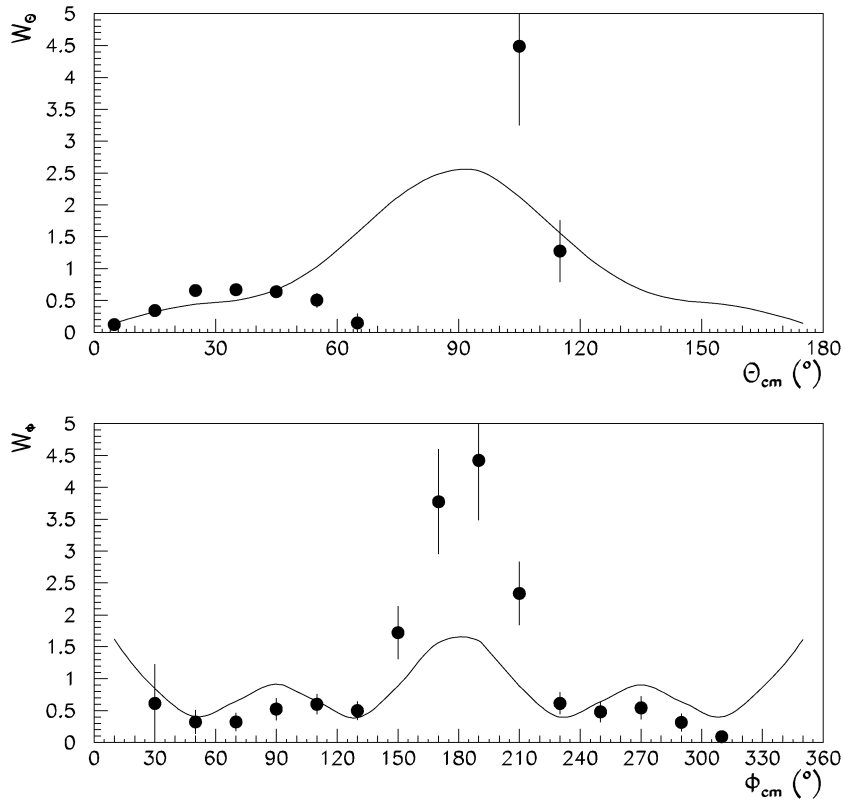

Fig. 4. The angular correlations W_θ (upper panel) and W_ϕ (lower panel) of the ^{12}C fragment for the 9.84-MeV resonance in the center-of-mass frame of the decaying ^{16}O and oriented in the direction of its velocity. (The α-particle correlation is at complementary angles.) The average θ and ϕ resolutions are about 15° and 20°, respectively.

1st derivative type is used that reproduces the measured B(E2) value for the respective transitions. This is folded with a projectile-nucleon interaction [19] to obtain the transition potential, which is used in the DWBA calculations. These results were also sampled with the setup efficiency but give yields more than 50% below the experimental values. Thus, we observe that the amplitude of the nuclear component depends on whether the deformed-potential or the folded-potential model is used. The data imply that the phenomenological deformed-potential model as implemented in ECIS gives a better description of the data in this case than the folding-potential model. In the future, this issue should be resolved by an independent test of the models on the 2^+_1 bound state in ^{16}O at 6.92 MeV, i.e., a measurement of the differential cross section under the same experimental conditions as for the unbound 2^+_2 and 2^+_3 states.

The current procedure is tailored to the case of 2^+ states and therefore no interference with E1 excitations is taken into account. For a continuum measurement, the Coulomb-excitation process and the fact that ^{16}O, ^{12}C and α are self-conjugate nuclei favor the quadrupole contribution. Nevertheless, the dipole part is present and must be measured and extracted. Our experiments show that in principle the E1–E2 interference pattern, which should lead to forward–backward asymmetry in the angular correlations, should also be measurable in the continuum via the fragment angular correlations, and thus permits a separation of both contributions. A better test could be done by measuring the two-dimensional correlation of the fragments instead of its projections on the $\theta_{\rm cm}$ and $\phi_{\rm cm}$ axes. This will require high statistics.

The next generation experiments could measure the continuum cross section and separate the E1

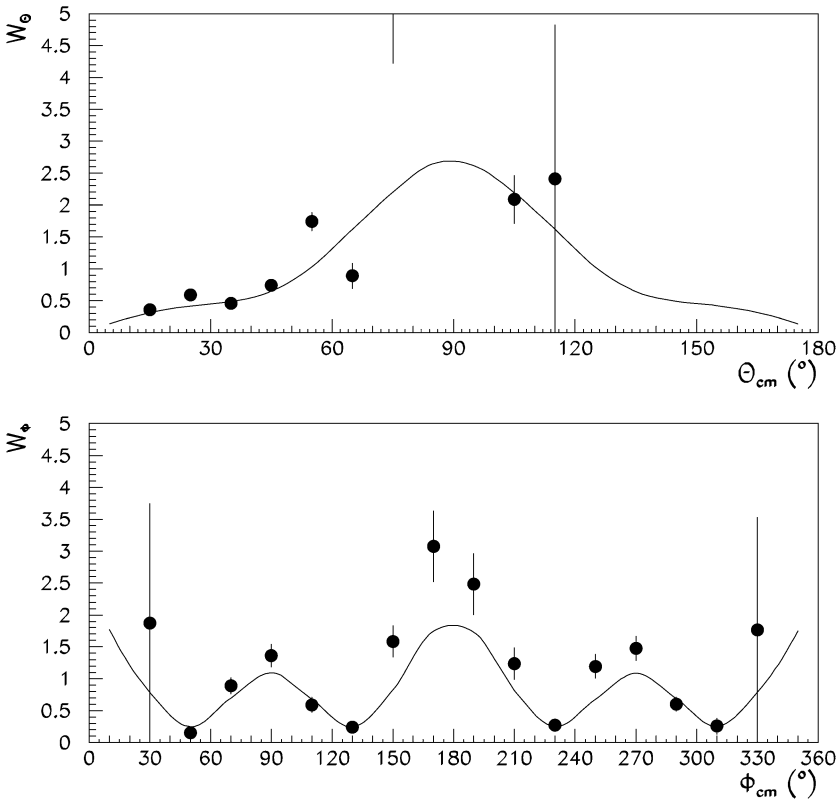

Fig. 5. Same as Fig. 4 but for the 11.52-MeV resonance. In the top figure, the data point at 75° has a value 14.3 ± 10.1.

and E2 components. A comparison with the direct-measurement data that exist at $\epsilon > 1$ MeV would be an ultimate verification of the Coulomb-dissociation method applied to the $^{12}C(\alpha,\gamma)^{16}O$ reaction. A measurement at $\epsilon < 1$ MeV where almost no data exist, would be accepted with more confidence. If the E1 component is sufficiently strong at low energy, also matching with the ^{16}N decay data [14,15] can be verified. In all cases the nuclear contribution will have to be checked by observing the differential cross section and correlations at scattering angles larger than 5° where the nuclear contribution is largely predominant.

Acknowledgements

This work has been performed as part of the research program of the *Stichting voor Fundamenteel Onderzoek der Materie* (FOM), with financial support from the *Nederlandse Organisatie voor Wetenschappelijk Onderzoek* (NWO).

References

[1] P. Dyer, C.A. Barnes, Nucl. Phys. A 233 (1974) 495.
[2] A. Redder, H.W. Becker, C. Rolfs, H.-P. Trautvetter, T.R. Donoghue, T.C. Rinckel, J.W. Hammer, K. Langanke, Nucl. Phys. A 462 (1987) 385.
[3] R.M. Kremer, C.A. Barnes, K.H. Chang, H.C. Evans, B.W. Filippone, K.H. Hahn, L.W. Mitchell, Phys. Rev. Lett. 60 (1988) 1475.
[4] J.M.L. Ouellet, M.N. Butler, H.C. Evans, H.W. Lee, J.R. Leslie, J.D. MacArthur, W. McLatchie, H.-B. Mak, P. Skensved, J.L. Whitton, X. Zhao, T.K. Alexander, Phys. Rev. C 54 (1996) 1982.
[5] G. Roters, C. Rolfs, F. Strieder, H.-P. Trautvetter, Eur. Phys. J. A 6 (1999) 451.
[6] L. Gialanella, D. Rogalla, F. Strieder, S. Theis, G. Gyrky, C. Agodi, M. Aliotta, L. Campajola, A. Del Zoppo, A. D'Onofrio, P. Figuera, U. Greife, G. Imbriani, A. Ordine, V. Roca, C. Rolfs, M. Romano, C. Sabbarese, P. Sapienza, F. Schmann, E. Somorjai, F. Terrasi, H.-P. Trautvetter, Eur. Phys. J. A 11 (2001) 357.
[7] R. Kunz, M. Jaeger, A. Mayer, J.W. Hammer, G. Staudt, S. Harissopulos, T. Paradellis, Phys. Rev. Lett. 86 (2001) 3244.
[8] G. Baur, M. Weber, Nucl. Phys. A 504 (1989) 352.

[9] T.D. Shoppa, S.E. Koonin, Phys. Rev. C 46 (1992) 382.
[10] V. Tatischeff, J. Kiener, P. Aguer, A. Lefebvre, Phys. Rev. C 51 (1995) 2789.
[11] V. Tatischeff, Ph.D. thesis, Universite de Caen, 1996, unpublished.
[12] D. O'Kelly, T. Botting, B. Hurst, R.P. Schmitt, Y.-W. Lui, Y. Hirabayashi, S. Okabe, Y. Sakuragi, H. Utsunomiya, T. Yamagata, M. Ohta, Phys. Lett. B 393 (1997) 301.
[13] G. Baur, K. Hencken, D. Trautmann, Prog. Part. Nucl. Phys. 51 (2003) 487.
[14] R.E. Azuma, L. Buchmann, F.C. Barker, C.A. Barnes, J.M. D'Auria, M. Dombsky, U. Giesen, K.P. Jackson, J.D. King, R.G. Korteling, P. McNeely, J. Powell, G. Roy, J. Vincent, T.R. Wang, S.S.M. Wong, P.R. Wrean, Phys. Rev. C 50 (1994) 1194.
[15] C.A. Barnes, Nucl. Phys. A 588 (1995) 295c.
[16] A.M. van den Berg, Nucl. Instrum. Methods B 99 (1995) 637.
[17] E. Plankl-Chabib, Ph.D. thesis, Universite d'Orsay, 1999, unpublished.
[18] J. Raynal, Notes on ECIS94, Report No. CEA-N-272, 1994, unpublished.
[19] F. Fleurot, Ph.D. thesis, Rijksuniversiteit Groningen, 2002, unpublished, http://www.ub.rug.nl/eldoc/dis/science/f.fleurot.
[20] M.N. Harakeh, A.R. Arends, M.J.A. de Voigt, A.G. Drentje, S.Y. van der Werf, A. van der Woude, Nucl. Phys. A 265 (1976) 189.
[21] P. Roussel-Chomaz, N. Alamanos, F. Auger, J. Barrette, B. Berthier, B. Fernandez, L. Papineau, Nucl. Phys. A 477 (1988) 345.
[22] F. Ajzenberg-Selove, Nucl. Phys. A 460 (1986) 1.